Proceedings of the Korean Nuclear Society Spring Meeting
Cheju, Korea, May 1996

Microscopic Study on the Laser Surface-Melted Alloy 600

Yun Soo Lim, Hai Dong Cho, Il Hiun Kuk and Joung Soo Kim
Korea Atomic Energy Research Institute

Abstract

Studies on the microstructural and compositional changes in sensitized Ni base Alloy 600 by laser surface melting have been carried out using TEM equipped with EDXA. The microstructure of the laser melted zone was mainly consisted of fine cells, and along the cell and grain boundaries, Cr enrichment due to its segregation was observed. Cr carbides having formed along the grain bundaries during the sensitization treatment have been completely dissloved. The cell walls were decorated with dislocations and the very tiny precipitates, found to be Ti(CN) type, were distributed randomly along the cell walls with tangled dislocations around them.

1. Introduction

Ni base Alloy 600 (commonly called Inconel 600*) is an austenite Ni-Cr-Fe alloy which is used extensively for tubing and other components in nuclear power plants. When thses alloys are heat treated at temperatures below the carbon solvus, Cr carbides are known to precipitate at the grain boundaries, causing Cr depletion along the boundaries. It renders the alloys susceptible to intergranular corrosion (IGC) and/or intergranular stress corrosion cracking (IGSCC) in some environments[1].

Since early 1980s, various types of lasers have been widely used to improve the surface properties of engineering materials. Laser beam has its own unique capabilities to material processing due to well controlled power density, non-contacting and precision processing, easy beam manipulation, so on. Moveover, since the laser treatment is restricted on the surface of the target material only, the properties of bulk material are not affected. From the previous experiments, it was proved that the surface treatments of sensitized Alloy 600[2], and sensitized stainless steels[3] by laser beam (laser surface melting) had improved the corrosion properties, especially IGSCC resistance. These results showed the possibilities for repair in the early stage of failure by crackings occurred in any tubes without great difficulties, since nowadays the laser beam processing can be carried out through optical fibers with a remote control system[4].

Obviously, improvement of the various material properties is caused by metallurgical changes, such as microstructural and/or compositional, occurring when laser beam interacts

with materials. After laser surface melting, newly re-solidified and heat affected regions around the surface are produced, and these metallurgical changes determine the properties of materials which are surface treated.

The purpose of this paper is to investigate the change of microstructure as well as the formation of new precipitates in IGSCC sensitized Alloy 600 by laser surface melting.

*Inconel is a trademark owned by the INCO family of companies.

2. Experimental Procedures

2.1 Materials and heat treatment

A plate, 1.6 mm in thickness, of commercially mill-annealed Ni base Alloy 600 was used in this study and the chemical composition of this alloy is listed in Table 1. Before laser surface melting, the specimens sealed in a quartz tube were solution annealed at 1050 ℃ for 30 min. and subsquently water cooled, followed by sensitization treatment at 600 ℃ for 24 hours in a vacuum furnace.

2.2 Laser surface melting

Laser surface melting of the sensitized specimens was carried out using a 4 kW CO_2 CW laser. Before laser melting, the specimens were polished on a 600 grit SiC paper to increase the absorption of laser beam. During laser treatment, a continuous flow of Ar (30 l/min) was blown onto the surface around the laser beam to prevent the melted region from oxidation. In Table 2, the important laser parameters used in this study are summarized. To get an area large enough to make TEM specimens, the specimens were scanned by overlapping the treated tracks by about half of the beam size.

2.3 Specimen preparation for microscopy

TEM, JEOL 2000FX II equipped with a Oxford Link Energy Dispersive X-ray Analyser, was used to examine the microstructures of the laser surface melted specimens, including micro-segregation of minor alloying elements as well as the size and distribution of the precipitates formed in the laser melted zone (LMZ) and the matrix. Thin foils were prepared by cross-sectioning the melted specimens to the slabs of 1 mm in thichness which were, afterward, thinned mechanically down to approximately 15 μm, followed by ion milling processs to get the final TEM specimens. In order to analyse the chemical compositions and the crystal structures of the precipitates having formed in the laser melted specimens, the carbon extraction replica technique was adopted with etching solution of 2% hydrochloric acid and 98% methanol for 15 sec at 6V.

SEM was also used to observe the shapes of the precipitates in the LMZ clearly. The specimens for SEM were made by deeply etching polished samples with the same etchant as that used for the carbon extraction replica.

3. Experimental Results and Discussion

3.1 The matrrix

Grain boundary carbides were fully developed and Cr depletion along the grain boundaries was occured under the sensitization treatment and Fig. 1 shows those grain boundary carbides. From SADP and EDS analyses of carbides, they were realized to be a mixture of $Cr_{23}C_6$ and Cr_7C_3. Besides these Cr carbides, sharply faceted inclusions were frequently found in the sensitized specimen. Fig. 2 shows these inclusions observed from an etched specimen under an optical microscope, the color of which was golden. it is believed that they should have been introduced during the fabrication of the alloy[5]. The EDX and SADP analyses from a carbon replica confirmed them to be TiN which is containing Cr as a minor element. Moreover, the TiN inclusions were not observed in the laser melted zone, as shown in Fig. 2, which indicates that TiN had been melted during laser melting. To be seen later, these melted TiN inclusions gave the characteristic microstructures and morphologies in the laser melted zone of this alloy.

3.2 The laser melted zone (LMZ)

TEM micrographs shown in Fig. 3 represent typical the microstructure of the laser melted zone. As seen in these Figures, the microstructure of the LMZ was (columnar) cellular. From SADPs, the melted zone was known to be composed of a single phase, fcc austenite, like that of the bulk matrix. The cell spacing was measured to be approximately 1.5 ㎛, the growth direction of which was always parallel to <100> which is a crystallographic growth direction of fcc crystals. From EDX analysis, it was revealed that the Cr content (18.5 wt%) along the cell boundaries was higher than that (15.3 wt%) in the cells or in the bulk matrix (15.9 wt%), while Ni content decreased to compenste the Cr enrichment. However, there was no noticable change in Fe content, which can be expected from the Ni-Cr and Ni-Fe phase diagrams[6]. This redistribution of the alloying elements was also observed along grain boundaries in the LMZ.

The cell walls were decorated with high density dislocations and had very small precipitates which were distributed randomly along the cell walls with tangled dislocations around them. The partical size was approximately up to 100 nm. Fig. 4 (a) shows precipitates in a carbon extraction replica, Fig. 4 (b), a ring pattern from those particles, which has a fcc structure a with lattice parameter of approximately 4.2 Å, and Fig. 4 (c), the representative EDX spectrum from one of those particles. The particles contained Ti as a major element and Cr, Nb, and Mg as minor elements. Here, it should be noted that all of these metal elements, except Mg, are strong carbide, nitride or carbo-nitride formers with very low free energies of formation. Therefore it could be concluded that the precipitates distributed along the cell and grain boundaries were a type of TiN or possibly Ti(CN). Since we performed surface melting only and there are no other sources for cell boundary precipitates, constitutes of precipitates in the cell boundaries were supplied from matrix itself in the LMZ, that is, from TiN inclusions as seen in that Fig. 2 existing in the matix before laser melting.

Fig. 5 shows SEM micrograph of particles in the LMZ. From this Figure, it can

be seen clearly that some single (faceted-) particles were agglomerated into big ones. The agglomerated ones seem to be formed due to collision between singe (faceted-) ones in the convective melt pool, in which the latter had already been formed, by the similar mechanism of the formation of larger SiO_2 inclusions due to collision between smaller ones in liquid iron[7,8]. Therefore those agglomerated ones would be an evidence that Ti(CN) type particles had already been formed in the liquid state of the matix. As solidification proceeds, these particles will be trapped eventually in the intercelluar regions with random distribution along the cell boundaries, as seen from TEM micrographs, Fig. 3. The high density dislocations on the cell boundaries seem to have been generated by thermal residual tensile stress during re-solidification in the LMZ with tanglling around particles entrapped along the cell boundaries.

4. Conclusion

From the microscopic investigation on the microstructures of the laser melted Alloy 600 specimens, we could get some results as follows in our experimental conditions:

1. Cr carbides of Cr_7C_3 and $Cr_{23}C_6$ were formed along the grain boundaries in the sensitized specimen, where Cr depletion occurred.
2. Cr carbides having formed earlier were completely melted out by laser surface melting
3. The microstructure of the LMZ consisted of fine cells with the tiny Ti(CN) type precipitates along the cell and grain boundaries.
4. The cells formed in the LMZ have the same phase as that of the matrix, which is fcc austenite. Cr element which has a low partition ratio to Ni, was segregated in the cell and grain boundaries in the LMZ, but Fe element was not.
5. Ti(CN) particles were formed and agglomerated in the convective melt pool, finally entrapped along the cell boundaries during solidification of the matrix.

References

1. E. Serra, EPRI Special Report NP-2114-SR, EPRI, Palo Alto, CA, 1981.
2. J. S. Kim, J. H. Suh and I. H. Kuk, Proc. Kor. Nuc. Soc. Autumn Meeting Vol. 2, pp 565, Korea Nuclear Society, Taejon, Korea (1994)
3. J. Stewart, D. B. Wells, P. M. Scott and A. S. Bransden, Corrosion, 46(8) 618 (1990)
4. Nucleonics Week, 34(21), 4 (1993)
5. T. L Lyman et al. (eds.), Atlas of Microstructures of Industrial Alloys pp. 315, Metals Handbook Vol. 7 (8th edition), American Society for Metals, Metals Park, Ohio (1972)
6. T. B. Massalski et al (eds.), Binary Alloy Phase Diagram Vol. 1, pp 842 (Cr-Ni), pp 1086 (Fe-Ni), American Society for Metals, Metals Park, Ohio (1986)
7. U. Lindborg and K. Torssell, Trans. TMS-AIME, 242, 95 (1968)
8. M. Myers and M. C. Flemings, Metall. Trans., 3, 2225 (1972)

Table 1. Chemical compositions of Alloy 600 (wt%)

Ni	Cr	Fe	C	S	Mo	Co	Si	Mn	Al	Cu	Ti	Nb	Mg	N
Bal.	15.9	7.6	0.04	0.002	0.25	0.38	0.15	0.17	0.12	0.22	0.21	tr.	0.008	0.04

Table 2. Laser parameters used in the experiments

Real laser power	500 W
Beam diameter	1 mm
Beam scanning rate	200 cm/min.
Scanning mode	Multi overlapped

Fig 1 BF image of a grain boundary in the sensitized Alloy 600

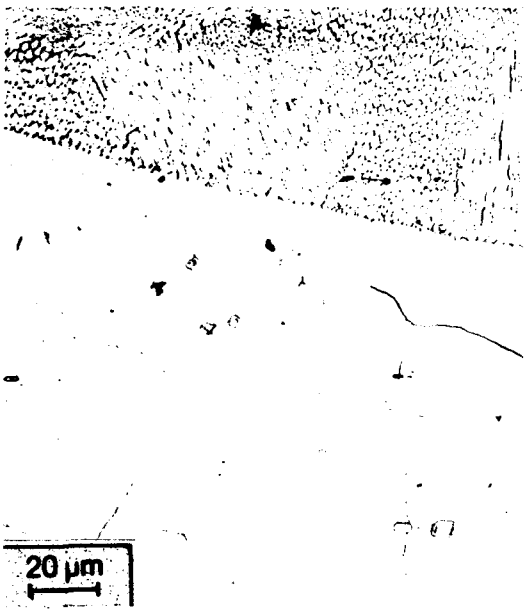

Fig 2 Optical micrograph of TiN inclusions in the laser surface melted Alloy 600

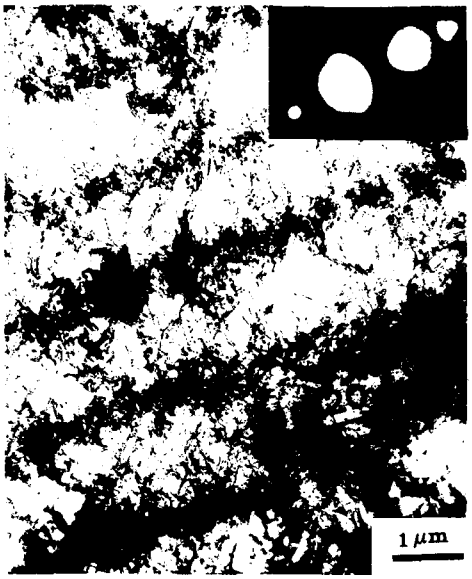

Fig. 3 BF image showing a cellular structure in the LMZ with **B** near [103]

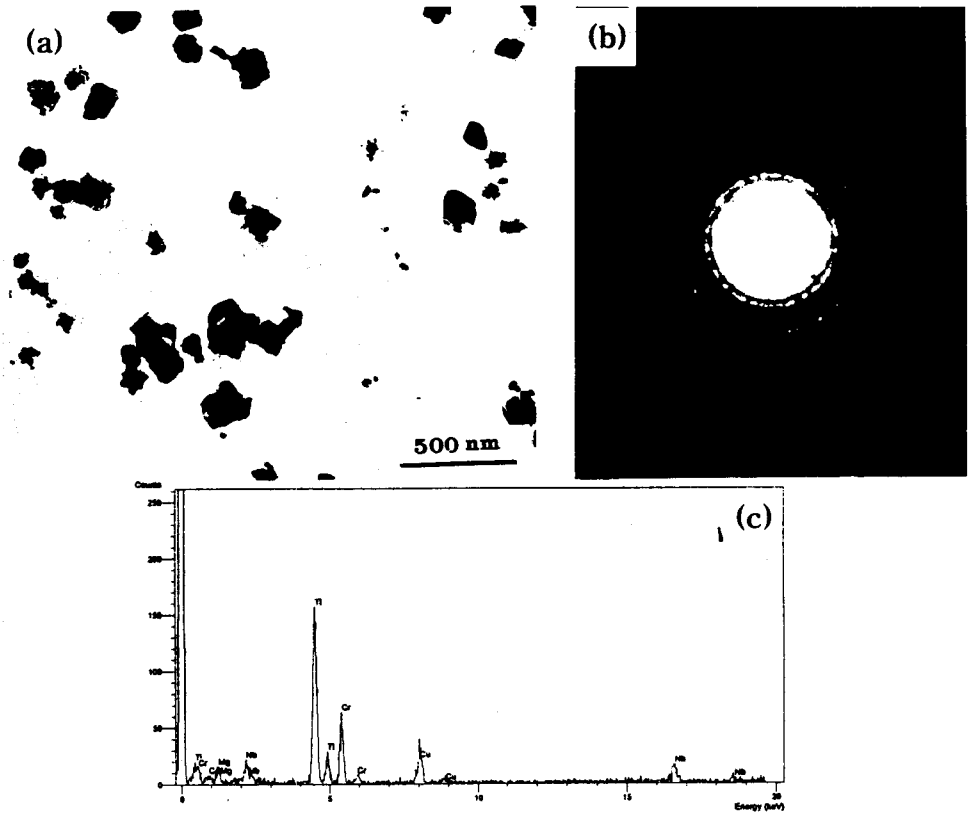

Fig. 4 BF image of particles in the LMZ (a), their related ring diffraction pattern (b) and EDX spectrum from one of those particles (c)

Fig. 5 SEM micrograph of particles in the LMZ from a etched specimen